

POINCARÉ GLOVE: HYPERBOLIC WORD EMBEDDINGS

Alexandru Țifrea*, Gary Bécigneul*, Octavian-Eugen Ganea*

Department of Computer Science

ETH Zürich, Switzerland

tifreaa@ethz.ch, {gary.becigneul, octavian.ganea}@inf.ethz.ch

ABSTRACT

Words are not created equal. In fact, they form an aristocratic graph with a latent hierarchical structure that the next generation of unsupervised learned word embeddings should reveal. In this paper, driven by the notion of delta-hyperbolicity or tree-likeness of a space, we propose to embed words in a Cartesian product of hyperbolic spaces which we theoretically connect with the Gaussian word embeddings and their Fisher distance. We adapt the well-known Glove algorithm to learn unsupervised word embeddings in this type of Riemannian manifolds. We explain how concepts from the Euclidean space such as parallel transport (used to solve analogy tasks) generalize to this new type of geometry. Moreover, we show that our embeddings exhibit hierarchical and hypernymy detection capabilities. We back up our findings with extensive experiments in which we outperform strong and popular baselines on the tasks of similarity, analogy and hypernymy detection.

1 INTRODUCTION & MOTIVATION

Word embeddings are ubiquitous nowadays as first layers in neural network and deep learning models for natural language processing. They are essential in order to move from the discrete word space to the continuous space where differentiable loss functions can be optimized. The popular models of Glove (Pennington et al., 2014), Word2Vec (Mikolov et al., 2013b) or FastText (Bojanowski et al., 2016), provide efficient ways to learn word vectors fully unsupervised from raw text corpora, solely based on word co-occurrence statistics. These models are then successfully applied to word similarity and other downstream tasks and, surprisingly (or not (Arora et al., 2016)), exhibit a linear algebraic structure that is also useful to solve word analogy.

However, unsupervised word embeddings still largely suffer from revealing asymmetric word relations including the latent hierarchical structure of words. This is currently one of the key limitations in automatic text understanding, e.g. for tasks such as textual entailment (Bowman et al., 2015). To address this issue, (Vilnis & McCallum, 2015; Muzellec & Cuturi, 2018) propose to move from point embeddings to probability density functions, the simplest being Gaussian or Elliptical distributions. Their intuition is that the variance of such a distribution should encode the generality/specificity of the respective word. However, this method results in losing the arithmetic properties of point embeddings (e.g. for analogy reasoning) and becomes unclear how to properly use them in downstream tasks. To this end, we propose to take the best from both worlds: we embed words as points in a Cartesian product of hyperbolic spaces and, additionally, explain how they are bijectively mapped to Gaussian embeddings with diagonal covariance matrices, where the hyperbolic distance between two points becomes the Fisher distance between the corresponding probability distribution functions (PDFs). We learn these embeddings unsupervised from raw text by generalizing the Glove method. Moreover, the linear arithmetic property used for solving word analogy has a mathematical grounded correspondence in this new space based on the notion of parallel transport. In addition, these hyperbolic embeddings exhibit hierarchical structure useful for hypernymy detection and outperform Euclidean Glove on word similarity benchmarks. Finally, they can be used as inputs for downstream tasks as explained in the recent work of Ganea et al. (2018b).

We provide additional reasons for choosing the hyperbolic geometry to embed words. We explain the notion of average δ -hyperbolicity of a graph, a geometric quantity that measures its "democracy" (Borassi et al., 2015). A small hyperbolicity constant implies "aristocracy", namely the existence of

*Equal contribution.

a small set of nodes that "influence" most of the paths in the graph. It is known that real-world graphs are mainly complex networks (e.g. scale-free exhibiting power-law node degree distributions) which in turn are better embedded in a tree-like space, i.e. hyperbolic (Krioukov et al., 2010). Since, intuitively, words form an "aristocratic" community (few generic ones from different topics and many more specific ones) and since a big subset of them exhibits a hierarchical structure (e.g. WordNet (Miller et al., 1990)), it is naturally to learn hyperbolic word embeddings. Moreover, we empirically measure very low average δ -hyperbolicity constants of some variants of the word log-co-occurrence graph (used by the Glove method), providing additional quantitative reasons for why spaces of negative curvature (i.e. hyperbolic) are better suited for word representations.

2 RELATED WORK

Recent *supervised methods* can be applied to embed any tree or directed acyclic graph in a low dimensional space with the aim of improving link prediction either by imposing a partial order in the embedding space (Vendrov et al., 2015; Vilnis et al., 2018; Athiwaratkun & Wilson, 2018), by using hyperbolic geometry (Nickel & Kiela, 2017; 2018), or both (Ganea et al., 2018a).

To learn *word embeddings* that exhibit hypernymy or hierarchical information, supervised methods (Vulić & Mrkšić, 2018; Nguyen et al., 2017) leverage external information (e.g. WordNet) together with raw text corpora. However, the same goal is also targeted by more ambitious fully unsupervised models which move away from the "point" assumption and learn various probability densities for each word (Vilnis & McCallum, 2015; Muzellec & Cuturi, 2018; Athiwaratkun & Wilson, 2017; Singh et al., 2018).

There have been two very recent attempts at learning unsupervised word embeddings in the hyperbolic space (Leimeister & Wilson, 2018; Dhingra et al., 2018). However, they suffer from either not being competitive on standard tasks in high dimensions, not showing the benefit of using hyperbolic spaces to model asymmetric relations, or not being trained on realistically large corpora. We address these problems and, moreover, the connection with density based methods is made explicit and leveraged to improve hypernymy detection.

3 HYPERBOLIC SPACES AND THEIR CARTESIAN PRODUCT

In order to work in the hyperbolic space, we have to choose one *model*, among the five isometric models that exist. We choose to embed words in the Poincaré ball $\mathbb{D}^n = \{x \in \mathbb{R}^n \mid \|x\|_2 < 1\}$. This is illustrated in Figure 1a for $n = 2$, where dark lines represent geodesics. The distance function in this space is given by $d_{\mathbb{D}^n}(x, y) = \cosh^{-1}(1 + \lambda_x \lambda_y \|x - y\|_2^2 / 2)$, $\lambda_x := 2/(1 - \|x\|_2^2)$ being the *conformal factor*. We will also embed words in products of

hyperbolic spaces, and explain why later on. A product of p balls $(\mathbb{D}^n)^p$, with the induced product geometry, is known to have distance function $d_{(\mathbb{D}^n)^p}(x, y)^2 = \sum_{i=1}^p d_{\mathbb{D}^n}(x_i, y_i)^2$. Finally, another model of interest for us is the Poincaré half-plane $\mathbb{H}^2 = \mathbb{R} \times \mathbb{R}_+^*$ illustrated in Figure 1d, with distance function $d_{\mathbb{H}^2}(x, y) = \cosh^{-1}(1 + \|x - y\|_2^2 / (2y_1 y_2))$. Figure 1 shows an isometry φ from \mathbb{D}^2 to \mathbb{H}^2 mapping the vertical segment $\{0\} \times (-1, 1)$ to \mathbb{R}_+^* and fixing $(0, 1)$, sending the radius to ∞ .

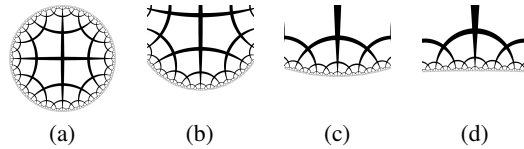


Figure 1: Isometric deformation φ of \mathbb{D}^2 into \mathbb{H}^2 .

4 ADAPTING GLOVE

Euclidean GLOVE. The GLOVE (Pennington et al., 2014) algorithm is an unsupervised method for learning word representations in the Euclidean space from statistics of word co-occurrences in a text corpus, with the aim to geometrically capture the words' meaning and relations.

We use the notations: X_{ij} is the number of times word j occurs in the same window context as word i ; $X_i = \sum_k X_{ik}$; $P_{ij} = X_{ij}/X_i$ is the probability that word j appears in the context of word i . An embedding of a (target) word i is written w_i , while an embedding of a context word k is written \tilde{w}_k .

The initial formulation of the GLOVE model suggests to learn embeddings as to satisfy the equation $w_i^T \tilde{w}_k = \log(P_{ik}) = \log(X_{ik}) - \log(X_i)$. Since X_{ik} is symmetric in (i, k) but P_{ik} is not, (Pennington et al., 2014) propose to restore the symmetry by introducing biases for each word, absorbing $\log(X_i)$ into i 's bias:

$$w_i^T \tilde{w}_k + b_i + \tilde{b}_k = \log(X_{ik}). \quad (1)$$

Finally, the authors suggest to enforce this equality by optimizing a weighted least-square loss:

$$J = \sum_{i,j=1}^V f(X_{ij}) \left(w_i^T \tilde{w}_j + b_i + \tilde{b}_j - \log X_{ij} \right)^2, \quad (2)$$

where V is the size of the vocabulary and f down-weights the signal coming from frequent words (it is typically chosen to be $f(x) = \min\{1, (x/x_m)^\alpha\}$, with $\alpha = 3/4$ and $x_m = 100$).

GLOVE in metric spaces. Note that there is no clear correspondence of the Euclidean inner-product in a hyperbolic space. However, we are provided with a distance function. Further notice that one could rewrite Eq. (1) with the Euclidean distance as $-\frac{1}{2}\|w_i - \tilde{w}_k\|^2 + b_i + \tilde{b}_k = \log(X_{ik})$, where we absorbed the squared norms of the embeddings into the biases. We thus replace the GLOVE loss by:

$$J = \sum_{i,j=1}^V f(X_{ij}) \left(-h(d(w_i, \tilde{w}_j)) + b_i + \tilde{b}_j - \log X_{ij} \right)^2, \quad (3)$$

where h is a function to be chosen as a hyperparameter of the model, and d can be any differentiable distance function. Although the most direct correspondence with GLOVE would suggest $h(x) = x^2/2$, we sometimes obtained better results with other functions, such as $h = \cosh^2$ (see sections 7 & 8). Note that De Sa et al. (2018) also apply \cosh to their distance matrix for hyperbolic MDS before applying PCA. Understanding why $h = \cosh^2$ is a good choice would be interesting future work.

5 CONNECTING GAUSSIAN EMBEDDINGS & HYPERBOLIC EMBEDDINGS

In order to endow Euclidean word embeddings with richer information, Vilnis & McCallum (2015) proposed to represent words as Gaussians, *i.e.* with a mean vector and a covariance matrix¹, expecting the variance parameters to capture how generic/specific a word is, and, hopefully, entailment relations. On the other hand, Nickel & Kiela (2017) proposed to embed words of the WordNet hierarchy (Miller et al., 1990) in hyperbolic space, because this space is mathematically known to be better suited to embed tree-like graphs. It is hence natural to wonder: is there a connection between the two?

The Fisher geometry of Gaussians is hyperbolic. It turns out that there exists a striking connection (Costa et al., 2015). Note that a *1D Gaussian* $\mathcal{N}(\mu, \sigma^2)$ can be represented as a point (μ, σ) in $\mathbb{R} \times \mathbb{R}_+^*$. Then, the Fisher distance between two distributions relates to the hyperbolic distance in \mathbb{H}^2 :

$$d_F(\mathcal{N}(\mu, \sigma^2), \mathcal{N}(\mu', \sigma'^2)) = \sqrt{2} d_{\mathbb{H}^2} \left((\mu/\sqrt{2}, \sigma), (\mu'/\sqrt{2}, \sigma') \right). \quad (4)$$

For n -dimensional Gaussians with diagonal covariance matrices written $\Sigma = \text{diag}(\sigma)^2$, it becomes:

$$d_F(\mathcal{N}(\mu, \Sigma), \mathcal{N}(\mu', \Sigma')) = \sqrt{\sum_{i=1}^n 2 d_{\mathbb{H}^2} \left((\mu_i/\sqrt{2}, \sigma_i), (\mu'_i/\sqrt{2}, \sigma'_i) \right)^2}. \quad (5)$$

Hence there is a direct correspondence between diagonal Gaussians and the product space $(\mathbb{H}^2)^n$.

¹diagonal or even spherical, for simplicity.

Fisher distance, KL & Gaussian embeddings. The above paragraph lets us relate the WORD2GAUSS algorithm (Vilnis & McCallum, 2015) to hyperbolic word embeddings. Although one could object that WORD2GAUSS is trained using a KL divergence, while hyperbolic embeddings relate to Gaussian distributions via the Fisher distance d_F , let us remind that KL and d_F define the same local geometry. Indeed, the KL is known to be related to d_F , as its local approximation (Jeffreys, 1946). In short, if $P(\theta + d\theta)$ and $P(\theta)$ denote two closeby probability distributions for a small $d\theta$, then $\text{KL}(P(\theta + d\theta) || P(\theta)) = (1/2) \sum_{ij} g_{ij} d\theta^i d\theta^j + \mathcal{O}(\|d\theta\|^3)$, where $(g_{ij})_{ij}$ is the Fisher information metric, inducing d_F .

Riemannian optimization. A benefit of representing words in (products of) hyperbolic spaces, as opposed to (diagonal) Gaussian distributions, is that one can use recent Riemannian adaptive optimization tools such as RADAGRAD (Bécigneul & Ganea, 2018). Note that without this connection, it would be unclear how to define a variant of ADAGRAD (Duchi et al., 2011) intrinsic to the statistical manifold of Gaussians. Empirically, we indeed noticed better results using RADAGRAD, rather than simply Riemannian SGD (Bonnabel, 2013). Similarly, note that GLOVE trains with ADAGRAD.

6 ANALOGIES AND ENTAILMENT FOR HYPERBOLIC/GAUSSIAN EMBEDDINGS

The connection exposed in section 5 allows us to provide mathematically grounded (i) analogy computations for Gaussian embeddings using hyperbolic geometry, and (ii) hypernymy detection for hyperbolic embeddings using Gaussian distributions.

6.1 COMPUTING ANALOGIES

A common task used to evaluate word embeddings, called *analogy*, consists in finding which word d is to the word c , what the word b is to the word a . For instance, *queen* is to *woman* what *king* is to *man*. In the Euclidean embedding space, the solution to this problem is usually taken geometrically as $d = c + (b - a) = b + (c - a)$. Note that the same d is also to b , what c is to a .

How should one intrinsically define “analogy parallelograms” in a space of Gaussian distributions? Note that Vilnis & McCallum (2015) do not evaluate their Gaussian embeddings on the analogy task, and that it would be unclear how to do so. However, since we can go back and forth between (diagonal) Gaussians and (products of) hyperbolic spaces as explained in section 5, we can use the fact that parallelograms are naturally defined in the Poincaré ball, by the notion of gyro-translation (Ungar, 2012, section 4). In the Poincaré ball, the two solutions $d_1 = c + (b - a)$ and $d_2 = b + (c - a)$ are respectively generalized to

$$d_1 = c \oplus \text{gyr}[c, \ominus a](\ominus a \oplus b), \quad \text{and} \quad d_2 = b \oplus \text{gyr}[b, \ominus a](\ominus a \oplus c). \quad (6)$$

The formulas for these operations are described in closed-forms in appendix C, and are easy to implement. The fact that d_1 and d_2 differ is due to the curvature of the space. For evaluation, we chose a point $m_{d_1 d_2}^t := d_1 \oplus ((-d_1 \oplus d_2) \otimes t)$ located on the geodesic between d_1 and d_2 for some $t \in [0, 1]$; if $t = 1/2$, this is called the *gyro-midpoint* and then $m_{d_1 d_2}^{0.5} = m_{d_2 d_1}^{0.5}$, which is at equal hyperbolic distance from d_1 as from d_2 . Note that one can rewrite Eq. (6) with tools from differential geometry as

$$c \oplus \text{gyr}[c, \ominus a](\ominus a \oplus b) = \exp_c(P_{a \rightarrow c}(\log_a(b))), \quad (7)$$

where $P_{x \rightarrow y} = (\lambda_x / \lambda_y) \text{gyr}[y, \ominus x]$ denotes the *parallel transport* along the unique geodesic from x to y . The exp and log maps of Riemannian geometry were related to the theory of gyrovector spaces (Ungar, 2008) by Ganea et al. (2018b), who also mention that when continuously deforming the hyperbolic space \mathbb{D}^n into the Euclidean space \mathbb{R}^n , sending the curvature from -1 to 0 (i.e. the radius of \mathbb{D}^n from 1 to ∞), the Möbius operations $\oplus^\kappa, \ominus^\kappa, \otimes^\kappa, \text{gyr}^\kappa$ recover their respective Euclidean counterparts $+, -, \cdot, Id$. Hence, the analogy solutions $d_1, d_2, m_{d_1 d_2}^t$ of Eq. (6) would then all recover $d = c + b - a$, which seems a nice sanity check.

6.2 A SCORE FOR ENTAILMENT/HYPERNYMY

Poincaré embeddings. Nickel & Kiela (2017) use a heuristic entailment score in order to predict whether u is a v , defined for $u, v \in \mathbb{D}^n$ as $\text{is-a}(u, v) := -(1 + \alpha(\|v\|_2 - \|u\|_2))d(u, v)$, where

$\alpha = 10^3$, based on the intuition that higher concepts in the hierarchy should be embedded with a lower Euclidean norm. However, such a choice is *not intrinsic* to the hyperbolic space. The loss that they use only for training involves the distance function, hence training is intrinsic to \mathbb{D}^n , *i.e.* invariant to applying any isometry $\varphi : \mathbb{D}^n \rightarrow \mathbb{D}^n$ to all word embeddings, but their “is-a” score is not.

The importance of fixing the isometry. We argue that generality of a concept as being embedded in a Poincaré ball is better captured by a *direction* in hyperbolic space, *i.e.* by a geodesic, rather than by the distance from the origin. Why? For a 1D Gaussian $\mathcal{N}(\mu, \sigma^2)$ representing a concept, generality should be naturally encoded in the magnitude of σ . As shown in section 5, we can map the space of Gaussians endorsed with the Fisher distance to the hyperbolic upper half-plane \mathbb{H}^2 , where σ corresponds to the (positive) second coordinate in $\mathbb{H}^2 = \mathbb{R} \times \mathbb{R}_+^*$. Moreover, as shown in section 3, \mathbb{H}^2 can be isometrically mapped to \mathbb{D}^2 , where the second coordinate $\sigma \in \mathbb{R}_+^*$ corresponds to the open vertical segment $\{0\} \times (-1, 1)$ in \mathbb{D}^2 . However, in \mathbb{D}^2 , any rotation w.r.t. the origin or any (hyperbolic) translation is an isometry². Hence, in order to map a word $x \in \mathbb{D}^2$ to a Gaussian $\mathcal{N}(\mu, \sigma^2)$ via \mathbb{H}^2 , we first have to align $\{0\} \times (-1, 1)$ with whichever geodesic in \mathbb{D}^2 encodes generality by applying the correct isometry to \mathbb{D}^2 (centering, rotation). These three steps are illustrated in Figure 2.

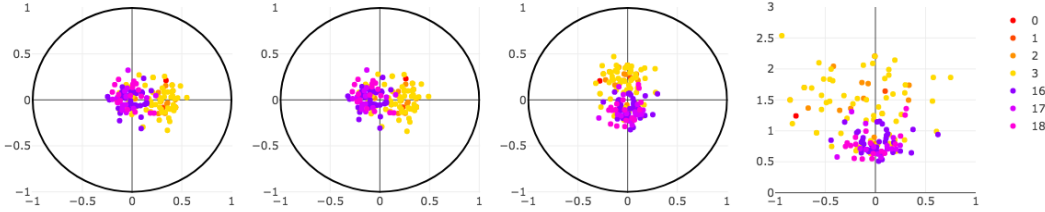


Figure 2: We show here one of the \mathbb{D}^2 spaces of 20D word embeddings embedded in $(\mathbb{D}^2)^{10}$ with our unsupervised hyperbolic GLOVE algorithm. This illustrates the three steps of applying the isometry. From left to right: the trained embeddings, raw; then after centering; then after rotation; finally after isometrically mapping them to \mathbb{H}^2 as explained in section 3. The isometry was obtained with the semi-supervised method described below, using 400 top/bottom words from WordNet. Legend: WordNet levels (root is 0). Model: $h = (\cdot)^2$, full vocabulary of 190k words. See more of these plots in appendix A.3.

Gaussian embeddings. Vilnis & McCallum (2015) propose using $\text{is-a}(P, Q) := -KL(P||Q)$ for distributions P, Q , the argument being that a low $KL(P||Q)$ indicates that we can encode Q easily as P , implying that Q entails P . However, we would like to mitigate this statement. Indeed, if $P = \mathcal{N}(\mu, \sigma)$ and $Q = \mathcal{N}(\mu, \sigma')$ are two 1D Gaussian distributions with same mean, then $KL(P||Q) = z^2 - 1 - \log(z)$ where $z := \sigma/\sigma'$, which is not a monotonic function of z . *This breaks the idea that the magnitude of the variance should encode the generality/specificity of the concept.*

Another entailment score for Gaussian embeddings. What would constitute a good number for the variance’s magnitude of a n -dimensional Gaussian distribution $\mathcal{N}(\mu, \Sigma)$? It is known that 95% of its mass is contained within a hyper-ellipsoid of volume $V_\Sigma = V_n \sqrt{\det(\Sigma)}$, where V_n denotes the volume of a ball of radius 1 in \mathbb{R}^n . For simplicity, we propose dropping the dependence in μ and define a simple score $\text{is-a}(\Sigma, \Sigma') := \log(V_{\Sigma'}) - \log(V_\Sigma) = \sum_{i=1}^n (\log(\sigma'_i) - \log(\sigma_i))$. Note that using difference of logarithms has the benefit of removing the scaling constant V_n , and makes the entailment score invariant to a rescaling of the covariance matrices: $\text{is-a}(r\Sigma, r\Sigma') = \text{is-a}(\Sigma, \Sigma'), \forall r > 0$.

Computing the score for hyperbolic embeddings. To compute our is-a score between two hyperbolic embeddings, we first map them to Gaussians and then apply the above proposed is-a score. However, as previously explained, in order to map a point $x \in (\mathbb{D}^n)^p$ to a diagonal Gaussian $\mathcal{N}(\mu, \Sigma)$, one first has to fix the correct isometry. To do so, we start by identifying two sets G and S of potentially generic and specific words, respectively. For the re-centering, we then compute the means g and s of G and S respectively, and $m := (s + g)/2$, and Möbius translate all words by the global mean with the operation $w \mapsto \ominus m \oplus w$. For the rotation, we set $u := (\ominus m \oplus g) / \|\ominus m \oplus g\|_2$, and

²See <http://bulatov.org/math/1001> for intuitive animations describing hyperbolic isometries.

rotate all words so that u is mapped to $(0, 1)$. Figure 2 illustrates these steps. In order to identify the two sets G and S , we propose (i) a fully unsupervised method, and (ii) a semi-supervised one, using a (varying) number of words from the WordNet hierarchy. In (i), we first define a restricted vocabulary of the 50k most frequent words among the unrestricted one of 190k words, and rank them by frequency; we then define G as the 5k most frequent ones, and S as the 5k least frequent ones of the 50k vocabulary (to avoid extremely rare words which might have received less signal during training). In (ii), we define G as k top words from the top 4 levels of the WordNet hierarchy, and S as k bottom words from the bottom 3 levels. Results are described in section 8: Figure 4 and Tables 6, 7.

7 EMBEDDING SYMBOLIC DATA IN A CONTINUOUS SPACE WITH MATCHING HYPERBOLICITY

Why would we embed words in a hyperbolic space? Given some symbolic data, such as a vocabulary along with similarity measures between words — in our case, co-occurrence counts X_{ij} — can we understand in a principled manner which geometry would represent it best? Choosing the right metric space to embed words can be understood as selecting the right inductive bias — an essential step.

δ -hyperbolicity. A particular quantity of interest describing qualitative aspects of metric spaces is the δ -hyperbolicity, introduced by Gromov (1987). However, for various reasons discussed in appendix B, we used the *averaged* δ -hyperbolicity, denoted δ_{avg} , defined by Albert et al. (2014). Intuitively, a low δ_{avg} of a finite metric space characterizes that this space has an underlying hyperbolic geometry, *i.e.* an approximate tree-like structure, and that the hyperbolic space would be well suited to isometrically embed it. We also report the ratio $2 * \delta_{avg} / d_{avg}$ (invariant to metric scaling), where d_{avg} is the average distance in the finite space, as suggested by Borassi et al. (2015), whose low value also characterizes the “hyperbolicity” of the space.

Computing δ_{avg} . Since our methods are trained on a weighted graph of co-occurrences, it makes sense to look for the corresponding hyperbolicity δ_{avg} of this symbolic data. However, in order to do so, one needs to be provided with a distance $d(i, j)$ for each pair of words (i, j) , while our symbolic data is only made of similarity measures. Note that one cannot simply associate the value $-\log(P_{ij})$ to $d(i, j)$, as this quantity is not symmetric. Instead, inspired from Eq. (3), we associate to words i, j the distance³ $h(d(i, j)) := -\log(X_{ij}) + b_i + b_j \geq 0$ with the choice $b_i := \log(X_i)$, *i.e.*

$$d(i, j) := h^{-1}(\log((X_i X_j) / X_{ij})). \quad (8)$$

Table 1 shows values for different choices of h . The discrete metric spaces we obtained for our symbolic data of co-occurrences appear to have a very low hyperbolicity, *i.e.* to be very much “hyperbolic”, which suggests to embed words in (products of) hyperbolic spaces. We report in section 8 empirical results for $h = (\cdot)^2$ and $h = \cosh^2$.

Table 1: average distances, δ -hyperbolicities and ratios computed via sampling for the metrics induced by different h functions, as defined in Eq. (8).

$h(x)$	d_{avg}	δ_{avg}	$2\delta_{avg}/d_{avg}$
$\log(x^2)$	18950.474	8498.6474	0.8969
x	18.9505	0.7685	0.0811
x^2	4.3465	0.088	0.0405
$\cosh(x)$	3.68	0.0384	0.0209
$\cosh^2(x)$	2.3596	0.0167	0.0142
$\cosh^3(x)$	1.9716	0.0102	0.0103
$\cosh^4(x)$	1.7918	0.0072	0.0081
$\cosh^5(x)$	1.6888	0.0056	0.0066
$\cosh^{10}(x)$	1.4947	0.0026	0.0034

³One can replace $\log(x)$ with $\log(1 + x)$ to avoid computing the logarithm of zero.

8 EXPERIMENTS: SIMILARITY, ANALOGY, ENTAILMENT

We now detail our experimental settings and results.

Experimental setup. We trained all models on a corpus provided by Levy & Goldberg (2014); Levy et al. (2015) used in other word embeddings related work. Corpus preprocessing is explained in the above references. The dataset has been obtained from an English Wikipedia dump and contains 1.4 billion tokens. Words appearing less than one hundred times in the corpus have been discarded, leaving 189,533 unique tokens. The co-occurrence matrix contains approximately 700 millions non-zero entries, for a symmetric window size of 10. All models were trained for 50 epochs, and unless stated otherwise, on the full corpus of 189,533 word types. For certain experiments, we also trained the model on a restricted vocabulary of the 50,000 most frequent words, which we specify by appending either “(190k)” or “(50k)” to the experiment’s name in the table of results.

Poincaré models, Euclidean baselines. We report results for both 100D embeddings trained in a 100D Poincaré ball, and for 50x2D embeddings, which were trained in the Cartesian product of 50 2D Poincaré balls. Note that in the case of both models, one word will be represented by a 100D array. For the Poincaré models we employ both $h(x) = x^2$ and $h(x) = \cosh^2(x)$.⁴ All hyperbolic models were optimized with RADAGRAD (Béginneul & Ganea, 2018). We compare against a 100D Euclidean GloVe model which was trained using the hyperparameters suggested in the original GloVe paper (Pennington et al., 2014). The vanilla GloVe model was optimized using ADAGRAD (Duchi et al., 2011). For the Euclidean baseline as well as for models with $h(x) = x^2$ we used a learning rate of 0.05. For Poincaré models with $h(x) = \cosh^2(x)$ we used a learning rate of 0.01.

A different initialization. For another experiment setting we initialize our Poincaré model with pretrained parameters. These were obtained by first training the same model on the restricted (50k) vocabulary, and using this model as an initialization. This will be referred to as the “initialization trick”. For fairness, we also trained the vanilla (Euclidean) GloVe model in the same fashion.

Similarity. Word similarity is assessed using a number of well established benchmarks shown in Table 2. We summarize here our main results, but more extensive experiments (including in lower dimensions) are in Appendix A.1.

Table 2: Word similarity results for 100-dimensional models.

Experiment name	Rare Word	WordSim	SimLex	SimVerb	MC	RG
100D Vanilla GloVe	0.3798	0.5901	0.2963	0.1675	0.6524	0.6894
100D Vanilla GloVe w/ init trick	0.3787	0.5668	0.2964	0.1639	0.6562	0.6757
100D Poincaré GloVe $h(x) = \cosh^2(x)$ w/ init trick	0.4187	0.6209	0.3208	0.1915	0.7833	0.7578
50x2D Poincaré GloVe $h(x) = \cosh^2(x)$	0.4111	0.6367	0.3084	0.1811	0.7748	0.725
50x2D Poincaré GloVe $h(x) = x^2$	0.4106	0.5844	0.3007	0.1725	0.7586	0.7236

Analogy. For word analogy, we evaluate on the Google benchmark (Mikolov et al., 2013a) and its two splits that contain semantic and syntactic analogy queries. We also use a benchmark by MSR that is also commonly employed in other word embedding works. For the Euclidean baselines we use 3COSADD (Levy et al., 2015). The solution d to the problem “which d is to c , what b is to a ” is selected as $m_{d_1 d_2}^t$, as described in section 6.1. In order to select the best t without overfitting on the benchmark dataset, we used the same 2-fold cross-validation method used by (Levy et al., 2015, section 5.1) (see our Table 15) – which resulted in selecting $t = 0.3$. We report our main results

⁴To be read as $(\cosh(x))^2$.

in Table 3, and more extensive experiments in various settings (including in lower dimensions) in appendix A.2.

Table 3: Word analogy results for 100-dimensional models.

Experiment name	Method	SemGoogle	SynGoogle	Google	MSR
100D Vanilla GloVe	3COSADD	0.6005	0.5869	0.5931	0.4868
100D Vanilla GloVe w/ init trick	3COSADD	0.6427	0.595	0.6167	0.4826
100D Poincaré GloVe $h(x) = \cosh^2(x)$, w/ init. trick	Cosine dist	0.6641	0.6088	0.6339	0.4971
50x2D Poincaré GloVe $h(x) = x^2$	Poincaré dist	0.6426	0.5940	0.6160	0.4576

Table 4: Nearest neighbors for some words for a 100D hyperbolic embedding model. Poincaré distance has been used for selecting neighbors.

sixties	seventies, eighties, nineties, 60s, 70s, 60s, 1960s, 80s, 90s, 70s
dance	dancing, dances, music, singing, musical, performing, hip-hop, pop, folk, dancers
daughter	wife, married, mother, cousin, son, niece, granddaughter, husband, sister, eldest
vapor	vapour, refrigerant, liquid, condenses, supercooled, fluid, gaseous, gases, droplet, ammonia
ronaldo	cristiano, ronaldinho, ronaldo, messi, zidane, romario, pele, zinedine, xavi, robinho
mechanic	electrician, fireman, machinist, welder, technician, builder, janitor, trainer, brakeman, fitter
algebra	algebras, homological, heyting, geometry, subalgebra, quaternion, calculus, mathematics, unital, algebraic

Table 5: Some words selected from the 100 nearest neighbors and ordered according to the hypernymy score function for a 50x2D hyperbolic embedding model using $h(x) = x^2$.

reptile	amphibians, carnivore, crocodilian, fish-like, dinosaur, alligator, triceratops
algebra	mathematics, geometry, topology, relational, invertible, endomorphisms, quaternions
music	performance, composition, contemporary, rock, jazz, electroacoustic, trio
feeling	sense, perception, thoughts, impression, emotion, fear, shame, sorrow, joy

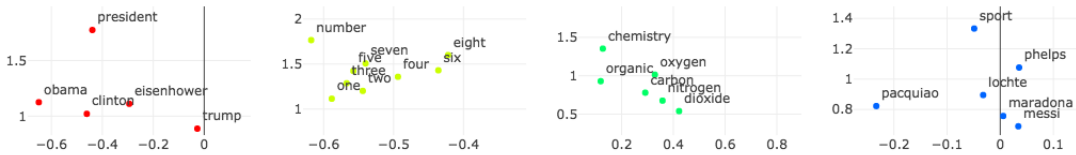


Figure 3: Different hierarchies captured by a 10x2D model with $h(x) = x^2$, in some selected 2D half-planes. Note how different 2D half-planes preserve certain semantic features better than others. The y coordinate encodes the magnitude of the variance, which represents generality/specificity.

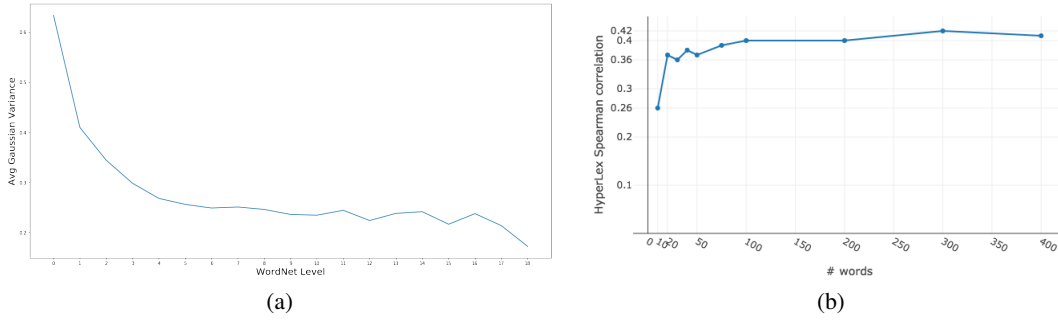


Figure 4: (4a): This plot describes how the Gaussian variances of our learned hyperbolic embeddings (trained unsupervised, isometry found with supervised information from WordNet) correlate with WordNet levels; (4b): This plot shows how the performance of our embeddings on hypernymy (HyperLex dataset) evolve when we increase the amount of supervision used to find the correct isometry. As can be seen, a very small amount of supervision (*e.g.* 20 words from WordNet) can significantly boost performance compared to fully unsupervised methods.

Hypernymy. For hypernymy evaluation we use the Hyperlex (Vulić et al., 2017) and WBLess (subset of BLess) (Baroni & Lenci, 2011) datasets. We compare against both strong supervised and unsupervised baselines. For Hyperlex we report results in Tab. 6 and use the baseline scores reported in (Nickel & Kiela, 2017; Vulić et al., 2017). For WBLess we report results in Tab. 7 and use the baseline scores reported in (Nguyen et al., 2017).

Our fully unsupervised methods outperform all their corresponding baselines, sometimes by a large margin. Our supervised methods achieve comparable scores with the best corresponding baselines, having the advantage of using much fewer labels, namely only 40 or 800 WordNet nodes, and only as a post-processing step (after training has finished) for identifying the best direction encoding the variance of the Gaussian distributions as described in Sec. 6.2.

Table 6: Hyperlex results. For each category (supervised or unsupervised) we highlight the top 2 performing methods.

Supervised methods	OrderEmb	0.191
	PARAGRAM + CF	0.32
	WN-Basic	0.24
	WN-WuP	0.214
	WN-LCh	0.214
	WN-Eucl from (Nickel & Kiela, 2017)	0.389
	WN-Poincare	0.512
Unsupervised methods	Word2Gauss-DistPos	0.206
	SGNS-Deps	0.205
	Frequency	0.279
	SLQS-Slim	0.229
	Vis-ID	0.253
Our models (semi-supervised and unsupervised)		
50x2D Poincaré GloVe, $h = \cosh^2$, (190k)	WordNet 20+20	0.359
	WordNet 400+400	0.411
	Unsupervised 5k+5k	0.277
50x2D Poincaré GloVe, $h = (\cdot)^2$, (190k)	WordNet 20+20	0.365
	WordNet 400+400	0.413
	Unsupervised 5k+5k	0.310
50x2D Poincaré GloVe, $h = \cosh^2$, (50k)	WordNet 20+20	0.368
	WordNet 400+400	0.412
	Unsupervised 5k+5k	0.295
50x2D Poincaré GloVe, $h = (\cdot)^2$, (50k)	WordNet 20+20	0.365
	WordNet 400+400	0.430
	Unsupervised 5k+5k	0.309

Table 7: WBLESS results. For each category (supervised or unsupervised) we highlight the top 2 performing methods.

Supervised methods	(Kiela et al., 2015)	0.75
	(Weeds et al., 2014)	0.75
	(Nguyen et al., 2017)	0.87
Unsupervised methods	SGNS from (Nguyen et al., 2017)	0.48
Our models		
50x2D Poincaré GloVe, $h = \cosh^2$, (190k)	WordNet 20+20	0.749
	WordNet 400+400	0.761
	Unsupervised 5k+5k	0.574
50x2D Poincaré GloVe, $h = (\cdot)^2$, (190k)	WordNet 20+20	0.771
	WordNet 400+400	0.76
	Unsupervised 5k+5k	0.647
50x2D Poincaré GloVe, $h = \cosh^2$, (50k)	WordNet 20+20	0.739
	WordNet 400+400	0.813
	Unsupervised 5k+5k	0.630
50x2D Poincaré GloVe, $h = (\cdot)^2$, (50k)	WordNet 20+20	0.752
	WordNet 400+400	0.810
	Unsupervised 5k+5k	0.649

9 CONCLUSION AND FUTURE WORK

We propose to adapt the GloVe algorithm to hyperbolic spaces and to leverage a connection between statistical manifolds of Gaussian distributions and hyperbolic geometry, in order to better interpret entailment relations between hyperbolic embeddings. We justify the choice of products of hyperbolic spaces via this connection to Gaussian distributions and via computations of the hyperbolicity of the symbolic data upon which GloVe is based. Future work includes jointly learning the curvature of the model, together with the h function defining the geometry from co-occurrence counts, as well as re-running experiments in the hyperboloid model, which has been reported to lead to lesser numerical instabilities.

REFERENCES

- Réka Albert, Bhaskar DasGupta, and Nasim Mobasher. Topological implications of negative curvature for biological and social networks. *Physical Review E*, 89(3):032811, 2014.
- Sanjeev Arora, Yuanzhi Li, Yingyu Liang, Tengyu Ma, and Andrej Risteski. A latent variable model approach to pmi-based word embeddings. *Transactions of the Association for Computational Linguistics*, 4:385–399, 2016.
- Ben Athiwaratkun and Andrew Wilson. Multimodal word distributions. In *Proceedings of the 55th Annual Meeting of the Association for Computational Linguistics (Volume 1: Long Papers)*, volume 1, pp. 1645–1656, 2017.
- Ben Athiwaratkun and Andrew Gordon Wilson. Hierarchical density order embeddings. *arXiv preprint arXiv:1804.09843*, 2018.
- Marco Baroni and Alessandro Lenci. How we blessed distributional semantic evaluation. In *Proceedings of the GEMS 2011 Workshop on GEometrical Models of Natural Language Semantics*, pp. 1–10. Association for Computational Linguistics, 2011.
- Gary Bécigneul and Octavian-Eugen Ganea. Riemannian adaptive optimization methods. *arXiv preprint arxiv:1810.00760*, 2018.
- Piotr Bojanowski, Edouard Grave, Armand Joulin, and Tomas Mikolov. Enriching word vectors with subword information. *arXiv preprint arXiv:1607.04606*, 2016.
- Silvère Bonnabel. Stochastic gradient descent on riemannian manifolds. *IEEE Transactions on Automatic Control*, 58(9):2217–2229, 2013.

-
- Michele Borassi, Alessandro Chessa, and Guido Caldarelli. Hyperbolicity measures democracy in real-world networks. *Physical Review E*, 92(3):032812, 2015.
- Samuel R Bowman, Gabor Angeli, Christopher Potts, and Christopher D Manning. A large annotated corpus for learning natural language inference. In *Proceedings of the 2015 Conference on Empirical Methods in Natural Language Processing*, pp. 632–642, 2015.
- Wei Chen, Wenjie Fang, Guangda Hu, and Michael W Mahoney. On the hyperbolicity of small-world and treelike random graphs. *Internet Mathematics*, 9(4):434–491, 2013.
- Sueli IR Costa, Sandra A Santos, and João E Strapasson. Fisher information distance: a geometrical reading. *Discrete Applied Mathematics*, 197:59–69, 2015. URL <https://arxiv.org/pdf/1210.2354.pdf>.
- Christopher De Sa, Albert Gu, Christopher Ré, and Frederic Sala. Representation tradeoffs for hyperbolic embeddings. In *International Conference on Machine Learning*, 2018.
- Bhuvan Dhingra, Christopher Shallue, Mohammad Norouzi, Andrew Dai, and George Dahl. Embedding text in hyperbolic spaces. In *Proceedings of the Twelfth Workshop on Graph-Based Methods for Natural Language Processing (TextGraphs-12)*, pp. 59–69, 2018.
- John Duchi, Elad Hazan, and Yoram Singer. Adaptive subgradient methods for online learning and stochastic optimization. *Journal of Machine Learning Research*, 12(Jul):2121–2159, 2011.
- Octavian-Eugen Ganea, Gary Bécigneul, and Thomas Hofmann. Hyperbolic entailment cones for learning hierarchical embeddings. In *International Conference on Machine Learning*, 2018a.
- Octavian-Eugen Ganea, Gary Bécigneul, and Thomas Hofmann. Hyperbolic neural networks. In *Advances in Neural Information Processing Systems*, 2018b.
- Mikhael Gromov. Hyperbolic groups. In *Essays in group theory*, pp. 75–263. Springer, 1987.
- Harold Jeffreys. An invariant form for the prior probability in estimation problems. *Proc. R. Soc. Lond. A*, 186(1007):453–461, 1946.
- Douwe Kiela, Laura Rimell, Ivan Vulić, and Stephen Clark. Exploiting image generality for lexical entailment detection. In *Proceedings of the 53rd Annual Meeting of the Association for Computational Linguistics and the 7th International Joint Conference on Natural Language Processing (Volume 2: Short Papers)*, volume 2, pp. 119–124, 2015.
- Dmitri Krioukov, Fragkiskos Papadopoulos, Maksim Kitsak, Amin Vahdat, and Marián Boguná. Hyperbolic geometry of complex networks. *Physical Review E*, 82(3):036106, 2010.
- Matthias Leimeister and Benjamin J Wilson. Skip-gram word embeddings in hyperbolic space. *arXiv preprint arXiv:1809.01498*, 2018.
- Omer Levy and Yoav Goldberg. Linguistic regularities in sparse and explicit word representations. In *Proceedings of the Eighteenth Conference on Computational Natural Language Learning*, pp. 171–180. Association for Computational Linguistics, 2014. doi: 10.3115/v1/W14-1618. URL <http://www.aclweb.org/anthology/W14-1618>.
- Omer Levy, Yoav Goldberg, and Ido Dagan. Improving distributional similarity with lessons learned from word embeddings. *Transactions of the Association for Computational Linguistics*, 3:211–225, 2015. ISSN 2307-387X. URL <https://transacl.org/ojs/index.php/tacl/article/view/570>.
- Tomas Mikolov, Kai Chen, Greg Corrado, and Jeffrey Dean. Efficient estimation of word representations in vector space. *arXiv preprint arXiv:1301.3781*, 2013a.
- Tomas Mikolov, Ilya Sutskever, Kai Chen, Greg S Corrado, and Jeff Dean. Distributed representations of words and phrases and their compositionality. In *Advances in neural information processing systems*, pp. 3111–3119, 2013b.

-
- George A Miller, Richard Beckwith, Christiane Fellbaum, Derek Gross, and Katherine J Miller. Introduction to wordnet: An on-line lexical database. *International journal of lexicography*, 3(4): 235–244, 1990.
- Boris Muzellec and Marco Cuturi. Generalizing point embeddings using the wasserstein space of elliptical distributions. *arXiv preprint arXiv:1805.07594*, 2018.
- Kim Anh Nguyen, Maximilian Köper, Sabine Schulte im Walde, and Ngoc Thang Vu. Hierarchical embeddings for hypernymy detection and directionality. In *Proceedings of the 2017 Conference on Empirical Methods in Natural Language Processing*, pp. 233–243, 2017.
- Maximilian Nickel and Douwe Kiela. Learning continuous hierarchies in the lorentz model of hyperbolic geometry. In *International Conference on Machine Learning*, 2018.
- Maximilian Nickel and Douwe Kiela. Poincaré embeddings for learning hierarchical representations. In *Advances in Neural Information Processing Systems*, pp. 6341–6350, 2017.
- Jeffrey Pennington, Richard Socher, and Christopher D Manning. Glove: Global vectors for word representation. In *EMNLP*, volume 14, pp. 1532–43, 2014.
- Sidak Pal Singh, Andreas Hug, Aymeric Dieuleveut, and Martin Jaggi. Wasserstein is all you need. *arXiv preprint arXiv:1808.09663*, 2018.
- Abraham A Ungar. *Beyond the Einstein addition law and its gyroscopic Thomas precession: The theory of gyrogroups and gyrovectors spaces*, volume 117. Springer Science & Business Media, 2012.
- Abraham Albert Ungar. A gyrovector space approach to hyperbolic geometry. *Synthesis Lectures on Mathematics and Statistics*, 1(1):1–194, 2008.
- Ivan Vendrov, Ryan Kiros, Sanja Fidler, and Raquel Urtasun. Order-embeddings of images and language. *arXiv preprint arXiv:1511.06361*, 2015.
- Luke Vilnis and Andrew McCallum. Word representations via gaussian embedding. *ICLR*, 2015.
- Luke Vilnis, Xiang Li, Shikhar Murty, and Andrew McCallum. Probabilistic embedding of knowledge graphs with box lattice measures. *arXiv preprint arXiv:1805.06627*, 2018.
- Ivan Vulić and Nikola Mrkšić. Specialising word vectors for lexical entailment. In *Proceedings of the 2018 Conference of the North American Chapter of the Association for Computational Linguistics: Human Language Technologies, Volume 1 (Long Papers)*, volume 1, pp. 1134–1145, 2018.
- Ivan Vulić, Daniela Gerz, Douwe Kiela, Felix Hill, and Anna Korhonen. Hyperlex: A large-scale evaluation of graded lexical entailment. *Computational Linguistics*, 43(4):781–835, 2017.
- Julie Weeds, Daoud Clarke, Jeremy Reffin, David Weir, and Bill Keller. Learning to distinguish hypernyms and co-hyponyms. In *Proceedings of COLING 2014, the 25th International Conference on Computational Linguistics: Technical Papers*, pp. 2249–2259. Dublin City University and Association for Computational Linguistics, 2014.

A MORE EXPERIMENTS

We show here extensive empirical results in various settings, including lower dimensions, different product structures, changing the vocabulary and using different h functions.

Experimental setup. In the experiment’s name, we first indicate which dimension was used: “ nD ” denotes \mathbb{D}^n while “ $p \times kD$ ” denotes $(\mathbb{D}^k)^p$. “Vanilla” designates the baseline, *i.e.* the standard Euclidean GloVe from Eq. (1), while “Poincaré” designates our hyperbolic GloVe from Eq. (3). For Poincaré models, we then append to the experiment’s name which h function was applied to distances during training. Every model was trained for 50 epochs. Vanilla models were optimized with Adagrad (Duchi et al., 2011) while Poincaré models were optimized with RADAGRAD (Bécigneul & Ganea, 2018). For each experiment we tried using learning rates in $\{0.01, 0.05\}$, and found that the best were 0.01 for $h = \cosh^2$ and 0.05 for $h = (\cdot)^2$ and for Vanilla models – accordingly, we only report the best results. For similarity, we only considered the “target word vector” and always ignored the “context word vector”. We also tried using the Euclidean/Möbius average⁵ of these, but obtained (almost) consistently worse results for all experiments (including baselines) and do not report them.

A.1 SIMILARITY

Reported scores are Spearman’s correlations on the ranks for each benchmark dataset, as usual in the literature. We used (minus) the Poincaré distance as a similarity measure to rank neighbors.

Table 8: Unrestricted (190k) similarity results: models were trained and evaluated on the unrestricted (190k) vocabulary – “(init)” refers to the fact that the model was initialized with its counterpart (*i.e.* with same hyperparameters) on the restricted (50k) vocabulary.

Experiment’s name	Rare Word	WordSim	SimLex	SimVerb	MC	RG
100D Glove						
100D Vanilla	0.3798	0.5901	0.2963	0.1675	0.6524	0.6894
100D Vanilla (init)	0.3787	0.5668	0.2964	0.1639	0.6562	0.6757
100D Poincaré, \cosh^2	0.3996	0.6486	0.3141	0.1777	0.7650	0.6834
100D Poincaré, \cosh^2 (init)	0.4187	0.6209	0.3208	0.1915	0.7833	0.7578
100D Poincaré, $(\cdot)^2$	0.3762	0.4851	0.2732	0.1563	0.6540	0.6024
50x2D Poincaré, \cosh^2	0.4111	0.6367	0.3084	0.1811	0.7748	0.7250
50x2D Poincaré, $(\cdot)^2$	0.4106	0.5844	0.3007	0.1725	0.7586	0.7236
48D Glove						
48D Vanilla	0.3497	0.5426	0.2525	0.1461	0.6213	0.6002
48D Poincaré, \cosh^2	0.3661	0.6040	0.2661	0.1539	0.7067	0.6466
48D Poincaré, $(\cdot)^2$	0.3574	0.4751	0.2418	0.1451	0.6780	0.6406
24x2D Poincaré, \cosh^2	0.3733	0.6020	0.2678	0.1513	0.7210	0.6595
24x2D Poincaré, $(\cdot)^2$	0.3825	0.5636	0.2655	0.1536	0.7857	0.6959
20D Glove						
20D Vanilla	0.2930	0.4412	0.2153	0.1153	0.5120	0.5367
20D Poincaré, \cosh^2	0.3139	0.4672	0.2147	0.1226	0.5372	0.5720
20D Poincaré, $(\cdot)^2$	0.3250	0.4227	0.1994	0.1182	0.5970	0.6188
10x2D Poincaré, \cosh^2	0.3239	0.4818	0.2329	0.1281	0.6028	0.5986
10x2D Poincaré, $(\cdot)^2$	0.3380	0.4785	0.2314	0.1239	0.6242	0.6349
4D Glove						
4D Vanilla	0.1445	0.1947	0.1356	0.0602	0.2701	0.3403
4D Poincaré, \cosh^2	0.1901	0.2424	0.1432	0.0581	0.2299	0.3065
4D Poincaré, $(\cdot)^2$	0.2031	0.2782	0.1395	0.0612	0.3173	0.3626

⁵A Möbius average is a gyro-midpoint, as explained in section 6.1.

Table 9: Restricted (50k) similarity results: models were trained and evaluated on the restricted (50k) vocabulary – except for the “Vanilla (190k)” baseline, which was trained on the unrestricted (190k) vocabulary and evaluated on the restricted vocabulary.

Experiment’s name	Rare Word	WordSim	SimLex	SimVerb	MC	RG
100D Glove						
100D Vanilla (190k)	0.4443	0.5986	0.3071	0.1705	0.7245	0.7114
100D Vanilla	0.4512	0.6091	0.2913	0.1742	0.6881	0.7148
100D Poincaré, \cosh^2	0.4606	0.6577	0.3156	0.1987	0.7916	0.7382
100D Poincaré, $(\cdot)^2$	0.4183	0.5241	0.2792	0.1671	0.6975	0.6753
50x2D Poincaré, \cosh^2	0.4661	0.6510	0.3152	0.2033	0.8098	0.7705
50x2D Poincaré, $(\cdot)^2$	0.4444	0.6009	0.3038	0.1858	0.7963	0.7862
48D Glove						
48D Vanilla	0.4299	0.6171	0.2777	0.1641	0.7262	0.6739
48D Poincaré, \cosh^2	0.4191	0.6070	0.2682	0.1694	0.7566	0.6973
48D Poincaré, $(\cdot)^2$	0.3808	0.4940	0.2449	0.1607	0.7334	0.6982
24x2D Poincaré, \cosh^2	0.4235	0.6044	0.2790	0.1636	0.7834	0.7294
24x2D Poincaré, $(\cdot)^2$	0.4121	0.5759	0.2703	0.1601	0.7911	0.7302
20D Glove						
20D Vanilla	0.3695	0.5198	0.2426	0.1271	0.6683	0.5960
20D Poincaré, \cosh^2	0.3683	0.4913	0.2255	0.1317	0.6627	0.6384
20D Poincaré, $(\cdot)^2$	0.3355	0.4125	0.2100	0.1240	0.6603	0.6556
10x2D Poincaré, \cosh^2	0.3749	0.4893	0.2321	0.1254	0.6775	0.6367
10x2D Poincaré, $(\cdot)^2$	0.3771	0.4748	0.2438	0.1396	0.6502	0.6461
4D Glove						
4D Vanilla	0.1744	0.2113	0.1470	0.0582	0.3227	0.3973
4D Poincaré, \cosh^2	0.2183	0.2799	0.1530	0.0745	0.4104	0.4548
4D Poincaré, $(\cdot)^2$	0.2265	0.2357	0.1273	0.0605	0.2784	0.3495

Remark. Note that restricting the vocabulary incurs a loss of certain pairs of words from the benchmark similarity datasets, hence similarity results on the restricted (50k) vocabulary from Table 9 should be analyzed with caution, and in the light of Tables 10 and 11 (especially for Rare Word).

Table 10: Percentage of word pairs that are dropped when replacing the unrestricted vocabulary of 190k words with the restricted one of the 50k most frequent words.

	Rare Word	WordSim	SimLex	SimVerb	MC	RG
%	67.55	0.84	1.00	9.85	3.33	6.15

Table 11: Initial number of word pairs in each benchmark similarity dataset.

	Rare Word	WordSim	SimLex	SimVerb	MC	RG
#	2034	353	999	3500	30	65

A.2 ANALOGY

Details and notations. In the column “method”, “3.c.a” denotes using 3COSADD to solve analogies, which was used for all Euclidean baselines; for Poincaré models, as explained in section 8, the solution to the analogy problem is computed as $m_{d_1 d_2}^t$ with $t = 0.3$, and then the nearest neighbor in the vocabulary is selected either with the Poincaré distance on the corresponding space, which we denote as “ d ”, or with cosine similarity on the full vector, which we denote as “cos”. Finally, note that each cell contains two numbers, designated by w and $w + \tilde{w}$ respectively: w denotes ignoring the context vectors, while $w + \tilde{w}$ denotes considering as our embeddings the Euclidean/Möbius average between the target vector w and the context vector \tilde{w} . In each dimension, we bold best results for w .

Table 12: Unrestricted (190k) analogy results: models were trained and evaluated on the unrestricted (190k) vocabulary – “(init)” refers to the fact that the model was initialized with its counterpart (*i.e.* with same hyperparameters) on the restricted (50k) vocabulary.

Experiment’s name	Method	Semantic Google analogy accuracy using $w/w + \tilde{w}$	Syntactic Google analogy accuracy using $w/w + \tilde{w}$	Total Google analogy accuracy using $w/w + \tilde{w}$	MSR analogy accuracy using $w/w + \tilde{w}$
100D Glove					
100D Vanilla	3.c.a	0.6005 / 0.6374	0.5869 / 0.5540	0.5931 / 0.5918	0.4868 / 0.4427
100D Vanilla (init)	3.c.a	0.6427 / 0.6878	0.5950 / 0.5672	0.6167 / 0.6219	0.4826 / 0.4509
100D Poincaré, cosh ²	d	0.4289 / 0.4444	0.5892 / 0.5484	0.5165 / 0.5012	0.4625 / 0.4186
	cos	0.4834 / 0.4908	0.5736 / 0.5514	0.5326 / 0.5239	0.4833 / 0.4395
100D Poincaré, cosh ² (init)	d	0.6010 / 0.6308	0.6121 / 0.5659	0.6070 / 0.5954	0.4793 / 0.4375
	cos	0.6641 / 0.6776	0.6088 / 0.5740	0.6339 / 0.6210	0.4971 / 0.4600
100D Poincaré, (\cdot) ²	d	0.1013 / 0.5110	0.2388 / 0.4865	0.1764 / 0.4976	0.1461 / 0.3235
	cos	0.4329 / 0.7152	0.2507 / 0.4596	0.3334 / 0.5756	0.2042 / 0.3628
50x2D Poincaré, cosh ²	d	0.4511 / 0.4745	0.5766 / 0.5365	0.5196 / 0.5083	0.4763 / 0.4268
	cos	0.3274 / 0.3553	0.4326 / 0.3924	0.3849 / 0.3756	0.3329 / 0.2914
50x2D Poincaré, (\cdot) ²	d	0.6426 / 0.6709	0.5940 / 0.5560	0.6160 / 0.6081	0.4576 / 0.4166
	cos	0.4754 / 0.5255	0.4544 / 0.4271	0.4639 / 0.4718	0.3425 / 0.2980
48D Glove					
48D Vanilla	3.c.a	0.3642 / 0.3650	0.451 / 0.4156	0.4115 / 0.3927	0.3467 / 0.3139
48D Poincaré, cosh ²	d	0.2368 / 0.2403	0.4693 / 0.4242	0.3638 / 0.3407	0.3755 / 0.3255
	cos	0.2479 / 0.2449	0.4704 / 0.4264	0.3694 / 0.3440	0.3919 / 0.3405
48D Poincaré, (\cdot) ²	d	0.2108 / 0.4575	0.2752 / 0.4452	0.2460 / 0.4508	0.1842 / 0.2790
	cos	0.4513 / 0.5848	0.3137 / 0.4334	0.3762 / 0.5021	0.2386 / 0.3232
24x2D Poincaré, cosh ²	d	0.2338 / 0.2412	0.4509 / 0.4116	0.3524 / 0.3343	0.3426 / 0.3039
	cos	0.1294 / 0.1445	0.2240 / 0.1971	0.1811 / 0.1733	0.1619 / 0.1427
24x2D Poincaré, (\cdot) ²	d	0.4663 / 0.4851	0.4834 / 0.4482	0.4756 / 0.4650	0.3456 / 0.3124
	cos	0.2479 / 0.2477	0.2626 / 0.2445	0.2559 / 0.2460	0.1670 / 0.1388
20D Glove					
20D Vanilla	3.c.a	0.1234 / 0.1202	0.2133 / 0.2004	0.1724 / 0.1640	0.1481 / 0.1281
20D Poincaré, cosh ²	d	0.1043 / 0.1020	0.2159 / 0.1946	0.1653 / 0.1526	0.1751 / 0.1527
	cos	0.1027 / 0.0993	0.2184 / 0.1955	0.1659 / 0.1519	0.1781 / 0.1505
20D Poincaré, (\cdot) ²	d	0.1728 / 0.1840	0.2717 / 0.2646	0.2268 / 0.2280	0.1580 / 0.1451
	cos	0.2133 / 0.2018	0.2950 / 0.2762	0.2579 / 0.2424	0.1821 / 0.1611
10x2D Poincaré, cosh ²	d	0.1005 / 0.1015	0.2102 / 0.1915	0.1604 / 0.1506	0.1570 / 0.1365
	cos	0.0424 / 0.0392	0.0773 / 0.0686	0.0615 / 0.0553	0.0520 / 0.0446
10x2D Poincaré, (\cdot) ²	d	0.1635 / 0.1618	0.2530 / 0.2263	0.2124 / 0.1970	0.1580 / 0.1446
	cos	0.0599 / 0.0548	0.0992 / 0.0861	0.0814 / 0.0719	0.0501 / 0.0408
4D Glove					
4D Vanilla	3.c.a	0.0036 / 0.0045	0.0012 / 0.0015	0.0023 / 0.0028	0.0011 / 0.0012
4D Poincaré, cosh ²	d	0.0089 / 0.0092	0.0043 / 0.0041	0.0064 / 0.0064	0.0046 / 0.0054
	cos	0.0036 / 0.0039	0.0020 / 0.0026	0.0027 / 0.0032	0.0015 / 0.0016
4D Poincaré, (\cdot) ²	d	0.0135 / 0.0133	0.0058 / 0.0061	0.0093 / 0.0094	0.0051 / 0.0056
	cos	0.0045 / 0.0050	0.0024 / 0.0029	0.0034 / 0.0038	0.0015 / 0.0011

Table 13: Restricted (50k) analogy results: models were trained and evaluated on the restricted (50k) vocabulary – except for the “Vanilla (190k)” baseline, which was trained on the unrestricted (190k) vocabulary and evaluated on the restricted vocabulary.

Experiment’s name	Method	Semantic Google analogy accuracy using $w/w + \tilde{w}$	Syntactic Google analogy accuracy using $w/w + \tilde{w}$	Total Google analogy accuracy using $w/w + \tilde{w}$	MSR analogy accuracy using $w/w + \tilde{w}$
100D Glove					
100D Vanilla (190k)	3.c.a	0.4789 / 0.4966	0.5684 / 0.5450	0.5278 / 0.5230	0.4382 / 0.3990
100D Vanilla	3.c.a	0.2848 / 0.3043	0.5003 / 0.5103	0.4025 / 0.4168	0.3545 / 0.3655
100D Poincaré, \cosh^2	d	0.3684 / 0.3803	0.5820 / 0.5545	0.4851 / 0.4754	0.4394 / 0.3970
	cos	0.3982 / 0.4014	0.5786 / 0.5504	0.4968 / 0.4828	0.4494 / 0.4016
100D Poincaré, $(\cdot)^2$	d	0.1265 / 0.4005	0.2209 / 0.4693	0.1781 / 0.4381	0.1384 / 0.3066
	cos	0.2634 / 0.5179	0.2521 / 0.4460	0.2572 / 0.4786	0.1933 / 0.3354
50x2D Poincaré, \cosh^2	d	0.3956 / 0.4012	0.5799 / 0.5451	0.4963 / 0.4798	0.4482 / 0.3957
	cos	0.2809 / 0.2789	0.4146 / 0.4067	0.3539 / 0.3488	0.3464 / 0.2880
50x2D Poincaré, $(\cdot)^2$	d	0.5204 / 0.5275	0.5819 / 0.5518	0.5540 / 0.5407	0.4404 / 0.3980
	cos	0.3873 / 0.4172	0.4517 / 0.4411	0.4225 / 0.4303	0.3335 / 0.2933
48D Glove					
48D Vanilla	3.c.a	0.3212 / 0.3299	0.4727 / 0.4303	0.4039 / 0.3847	0.3550 / 0.3156
48D Poincaré, \cosh^2	d	0.2127 / 0.2163	0.4680 / 0.4239	0.3521 / 0.3297	0.3581 / 0.3078
	cos	0.2180 / 0.2220	0.4690 / 0.4228	0.3551 / 0.3317	0.3708 / 0.3134
48D Poincaré, $(\cdot)^2$	d	0.2035 / 0.3676	0.2572 / 0.4129	0.2329 / 0.3923	0.1787 / 0.2652
	cos	0.3063 / 0.4212	0.3090 / 0.4174	0.3078 / 0.4192	0.2243 / 0.2951
24x2D Poincaré, \cosh^2	d	0.2307 / 0.2308	0.4506 / 0.4090	0.3508 / 0.3281	0.3289 / 0.2979
	cos	0.1328 / 0.1334	0.2475 / 0.2153	0.1955 / 0.1781	0.1850 / 0.1544
24x2D Poincaré, $(\cdot)^2$	d	0.3649 / 0.3788	0.4738 / 0.4343	0.4244 / 0.4091	0.3424 / 0.2985
	cos	0.2041 / 0.2080	0.2680 / 0.2469	0.2390 / 0.2293	0.1805 / 0.1611
20D Glove					
20D Vanilla	3.c.a	0.1223 / 0.1164	0.2472 / 0.2120	0.1905 / 0.1686	0.1550 / 0.1289
20D Poincaré, \cosh^2	d	0.0925 / 0.0903	0.2292 / 0.1967	0.1672 / 0.1484	0.1601 / 0.1286
	cos	0.0917 / 0.0890	0.2355 / 0.1964	0.1702 / 0.1477	0.1629 / 0.1271
20D Poincaré, $(\cdot)^2$	d	0.1583 / 0.1661	0.2619 / 0.2479	0.2149 / 0.2108	0.1624 / 0.1419
	cos	0.1757 / 0.1777	0.2970 / 0.2613	0.2408 / 0.2220	0.1804 / 0.1554
10x2D Poincaré, \cosh^2	d	0.0962 / 0.0945	0.2177 / 0.1919	0.1626 / 0.1477	0.1546 / 0.1279
	cos	0.0403 / 0.0387	0.0850 / 0.0704	0.0647 / 0.0560	0.0483 / 0.0432
10x2D Poincaré, $(\cdot)^2$	d	0.1440 / 0.1467	0.2533 / 0.2231	0.2037 / 0.1884	0.1580 / 0.1417
	cos	0.0614 / 0.0583	0.1014 / 0.0880	0.0832 / 0.0745	0.0473 / 0.0435
4D Glove					
4D Vanilla	3.c.a	0.0050 / 0.0053	0.0011 / 0.0012	0.0029 / 0.0031	0.0011 / 0.0011
4D Poincaré, \cosh^2	d	0.0054 / 0.0056	0.0037 / 0.0037	0.0045 / 0.0046	0.0041 / 0.0044
	cos	0.0038 / 0.0036	0.0023 / 0.0025	0.0030 / 0.0030	0.0006 / 0.0006
4D Poincaré, $(\cdot)^2$	d	0.0127 / 0.0127	0.0072 / 0.0077	0.0097 / 0.0100	0.0061 / 0.0057
	cos	0.0060 / 0.0061	0.0030 / 0.0037	0.0043 / 0.0048	0.0024 / 0.0025

Remark. Note that restricting the vocabulary to the most frequent 190k or 50k words will remove some of the test instances in the benchmark analogy datasets. These are described in Table 14.

Table 14: Number of test instances in the benchmark analogy datasets initially and after reductions to the vocabularies of the most frequent 190k and 50k words respectively.

	Semantic Google	Syntactic Google	Total Google	MSR
initial	8869	10675	19544	8000
190k	8649	10609	19258	7118
50k	6549	9765	16314	5778

Table 15: Result of the 2-fold cross-validation to determine which t is best in $m_{d_1 d_2}^t$ (see section 6.1) to answer analogy queries. The (total) Google analogy dataset was randomly split in two partitions. For each partition, we selected the best t across the 11 choices in $\{0, 0.1, 0.2, \dots, 1\}$, and reported the test accuracy for this t . For both partitions, best results were obtained with $t = 0.3$.

	Validation accuracy	Test accuracy
Validation on partition 1 Test on partition 2	63.91	64.75
Validation on partition 2 Test on partition 1	64.75	63.91

A.3 HYPERNYMY

We show here more plots illustrating the method (described in section 6.2) that we use to map points from a (product of) Poincaré disk(s) to a (diagonal) Gaussian. Colors indicate WordNet levels: low levels are closer to the root. Figures 5,6,7,8 show the three steps (centering, rotation, isometric mapping to half-plane) for 20D embeddings in $(\mathbb{D}^2)^{10}$, *i.e.* each of these steps in each of the 10 corresponding 2D spaces. In these figures, centering and rotation were determined with our proposed semi-supervised method, *i.e.* selecting 400+400 top and bottom words from the WordNet hierarchy. We show these plots for two models in $(\mathbb{D}^2)^{10}$: one trained with $h = (\cdot)^2$ and one with $h = \cosh^2$.

Remark. It is easily noticeable that words trained with $h = \cosh^2$ are embedded much closer to each other than those trained with $h = (\cdot)^2$. This is expected: h is applied to the distance function, and according to Eq. (3), $d(w_i, \tilde{w}_j)$ should match $h^{-1}(b_i + \tilde{b}_j - \log(X_{ij}))$, which is smaller for $h = \cosh^2$ than for $h = (\cdot)^2$.

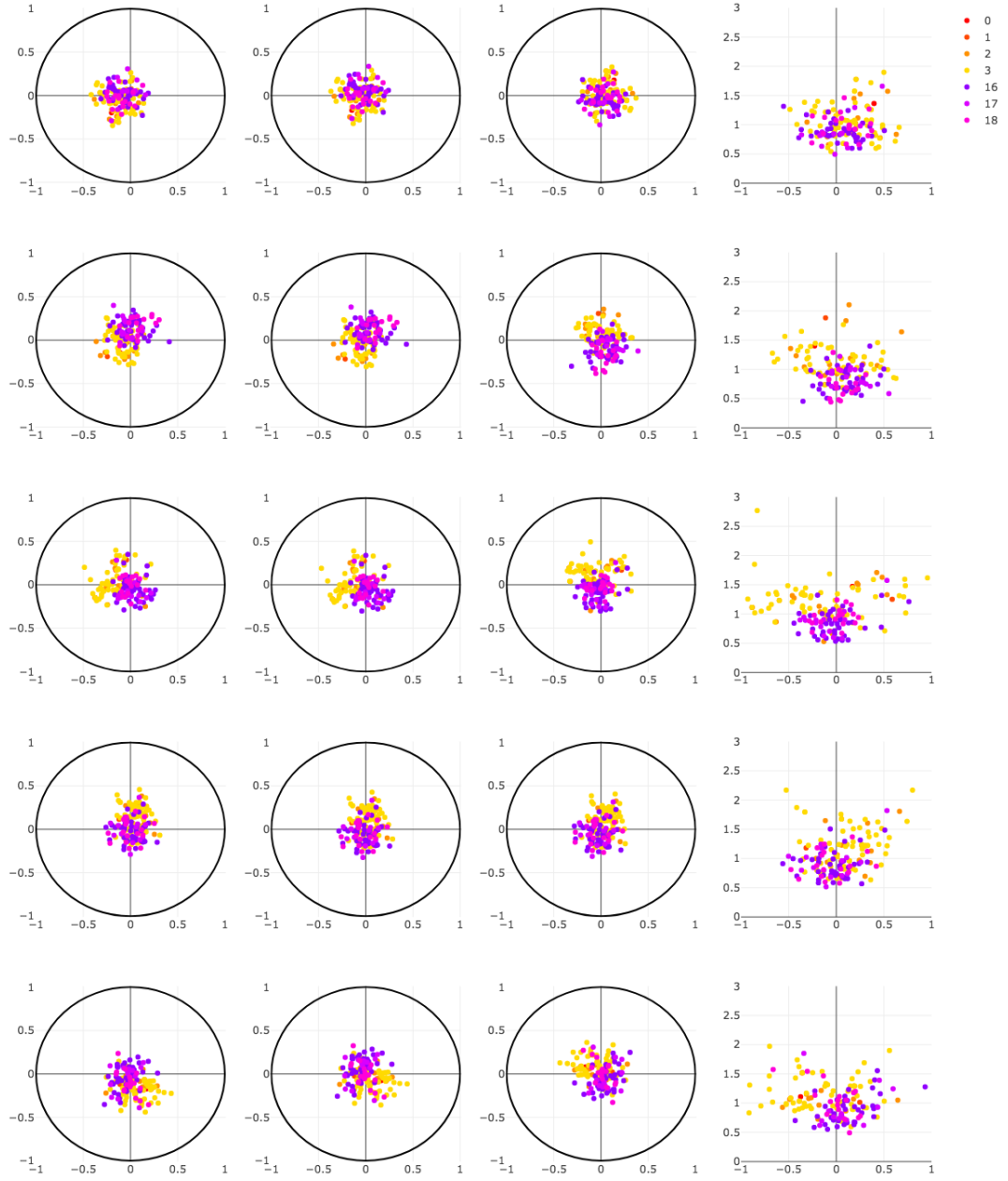


Figure 5: The first five 2D spaces of the model trained with $h = (\cdot)^2$.

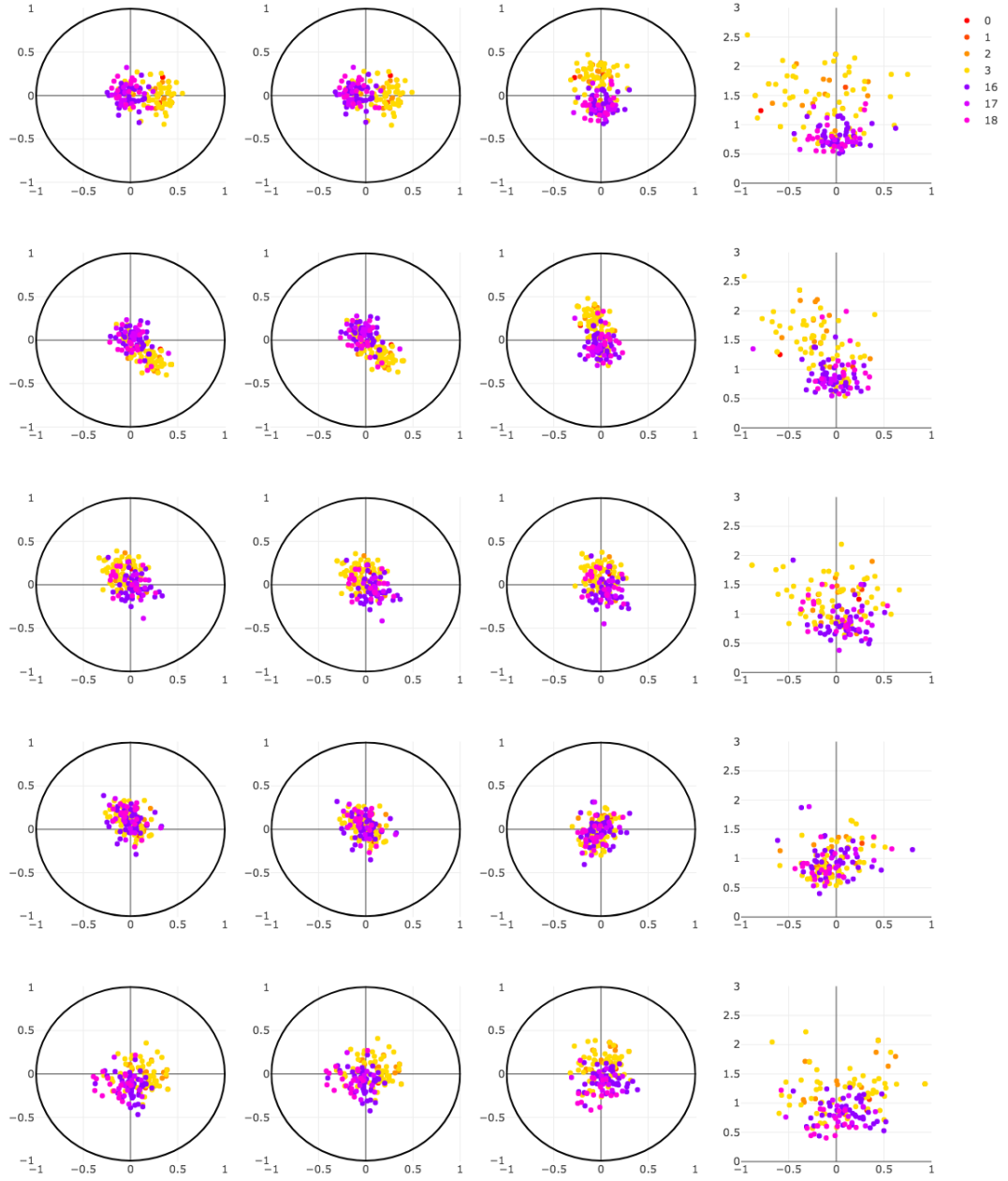


Figure 6: The last five 2D spaces of the model trained with $h = (\cdot)^2$.

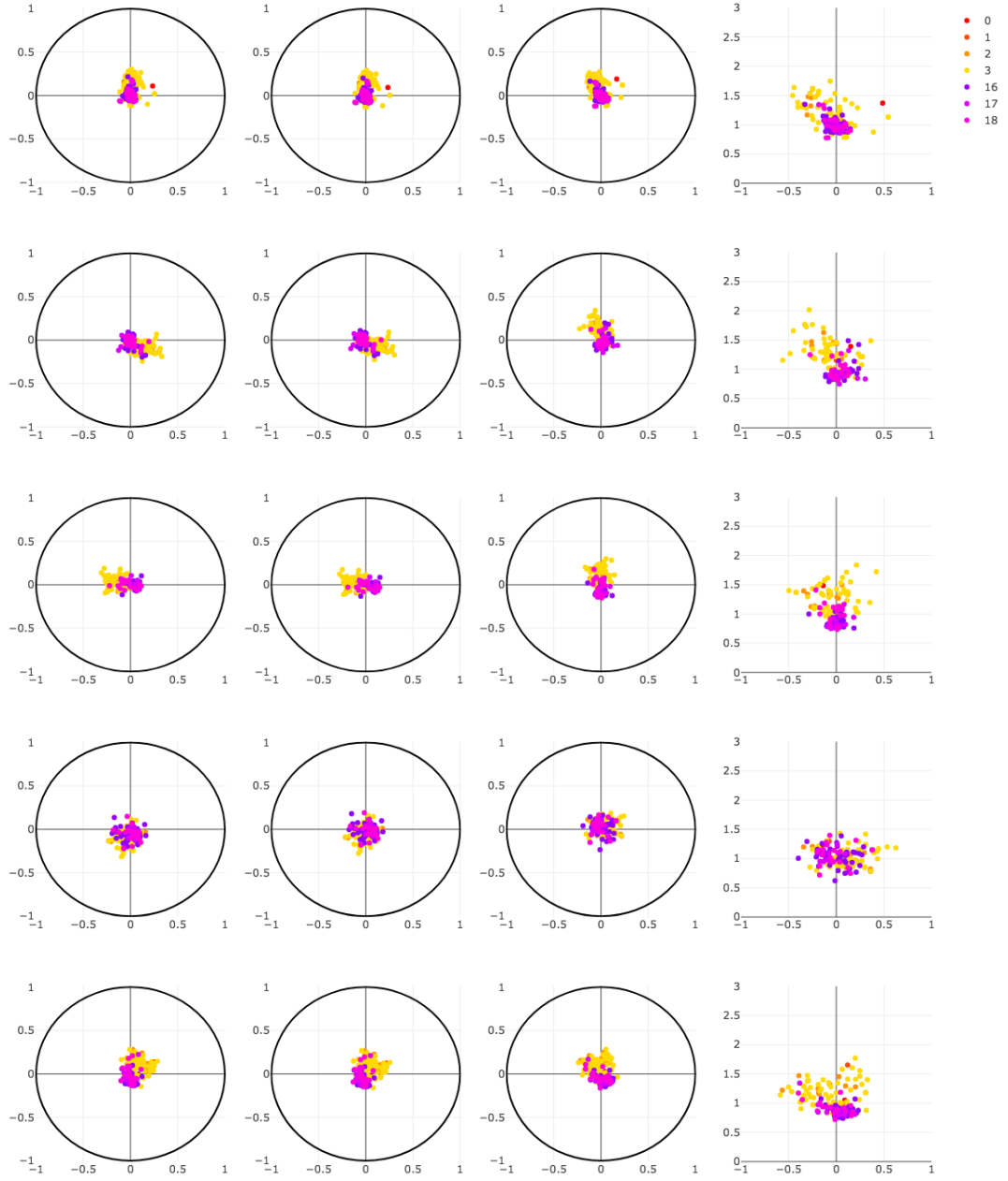


Figure 7: The first five 2D spaces of the model trained with $h = \cosh^2$.

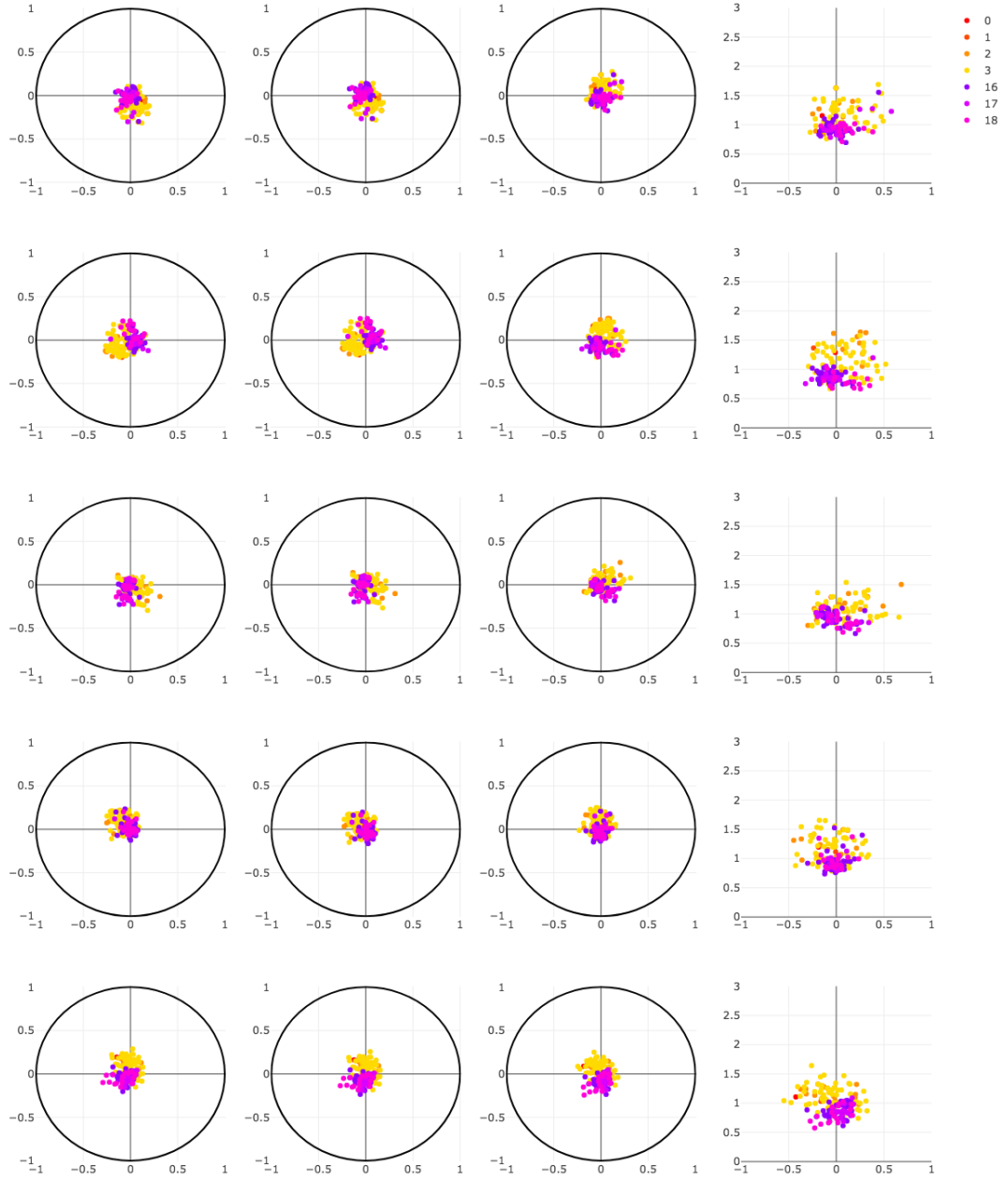


Figure 8: The last five 2D spaces of the model trained with $h = \cosh^2$.

B δ -HYPERBOLICITY

Let us start by defining the δ -hyperbolicity, introduced by Gromov (1987). The *hyperbolicity* $\delta(x, y, z, t)$ of a 4-tuple (x, y, z, t) is defined as half the difference between the biggest two of the following sums: $d(x, y) + d(z, t)$, $d(x, z) + d(y, t)$, $d(x, t) + d(y, z)$. The δ -hyperbolicity of a metric space is defined as the supremum of these numbers over all 4-tuples. Following Albert et al. (2014), we will denote this number by δ_{worst} , and by δ_{avg} the average of these over all 4-tuples, when the space is a finite set. An equivalent and more intuitive definition holds for geodesic spaces, *i.e.* when we can define triangles: its δ -hyperbolicity (δ_{worst}) is the smallest $\delta > 0$ such that for any triangle Δxyz , there exists a point at distance at most δ from each side of the triangle. Chen et al. (2013) and Borassi et al. (2015) analyzed δ_{worst} and δ_{avg} for specific graphs, respectively. A low hyperbolicity of a graph indicates that it has an underlying hyperbolic geometry, *i.e.* that it is approximately tree-like, or at least that there exists a taxonomy of nodes. Conversely, a high hyperbolicity of a graph suggests that it possesses long cycles, or could not be embedded in a low dimensional hyperbolic space without distortion. For instance, the Euclidean space \mathbb{R}^n is not δ -hyperbolic for any $\delta > 0$, and is hence described as ∞ -hyperbolic, while the Poincaré disk \mathbb{D}^2 is known to have a δ -hyperbolicity of $\log(1 + \sqrt{2}) \simeq 0.88$. On the other-hand, a product $\mathbb{D}^2 \times \mathbb{D}^2$ is ∞ -hyperbolic, because a 2D plane \mathbb{R}^2 could be isometrically embedded in it using for instance the first coordinates of each \mathbb{D}^2 . However, if \mathbb{D}^2 would constitute a good choice to embed some given symbolic data, then most likely $\mathbb{D}^2 \times \mathbb{D}^2$ would as well. This stems from the fact that δ -hyperbolicity (δ_{worst}) is a worst case measure which does not reflect what one could call the “hyperbolic capacity” of the space. Furthermore, note that computing δ_{worst} requires $\mathcal{O}(n^4)$ for a graph of size n , while δ_{avg} can be approximated via sampling. Finally, δ_{avg} is robust to adding/removing a node from the graph, while δ_{worst} is not. For all these reasons, we choose δ_{avg} as a measure of hyperbolicity.

More experiments. As explained in section 7, we computed hyperbolicities of the metric space induced by different h functions, on the matrix of co-occurrence counts, as reported in Table 1. We also conducted similarity experiments, reported in Table 17. Apart from WordSim, results improved for higher powers of cosh, corresponding to more hyperbolic spaces. However, also note that higher powers will tend to result in words embedded much closer to each other, *i.e.* with smaller distances, as explained in appendix A.3. In order to know whether this benefit comes from contracting distances or making the space more “hyperbolic”, it would be interesting to learn (or cross-validate) the curvature c of the Poincaré ball (or equivalently, its radius) jointly with the h function. Finally, in order to explain why WordSim behaved differently compared to other benchmarks, we investigated different properties of these, as reported in Table 16. The geometry of the words appearing in WordSim do not seem to have a different hyperbolicity compared to other benchmarks; however, WordSim seems to contain much more frequent words. Since hyperbolicities are computed with the assumption that $b_i = \log(X_i)$ (see Eq. (8)), it would be interesting to explore whether learned biases indeed take these values. We left this as future work.

Table 16: Various properties of similarity benchmark datasets. The frequency index indicates the rank of a word in the vocabulary in terms of its frequency: a low index describes a frequent word. The median of indexes seems to best discriminate WordSim from SimLex and SimVerb.

Property	WordSim	SimLex	SimVerb
# of test instances	353	999	3,500
# of different words	419	1,027	822
min. index (frequency)	57	38	21
max. index (frequency)	58,286	128,143	180,417
median of indexes	2,723	4,463	9,338
$\delta_{avg}, (\cdot)^2$	0.0738	0.0759	0.0799
δ_{avg}, \cosh^2	0.0154	0.0156	0.0164
$2\delta_{avg}/d_{avg}, (\cdot)^2$	0.0381	0.0384	0.0399
$2\delta_{avg}/d_{avg}, \cosh^2$	0.0136	0.0137	0.0143

Table 17: Similarity results on the unrestricted (190k) vocabulary for various h functions. This table should be read together with Table 1.

Experiment's name	Rare Word	WordSim	SimLex	SimVerb
100D Vanilla	0.3840	0.5849	0.3020	0.1674
100D Poincaré, cosh	0.3353	0.5841	0.2607	0.1394
100D Poincaré, cosh ²	0.3981	0.6509	0.3131	0.1757
100D Poincaré, cosh ³	0.4170	0.6314	0.3155	0.1825
100D Poincaré, cosh ⁴	0.4272	0.6294	0.3198	0.1845

C CLOSED-FORM FORMULAS OF MÖBIUS OPERATIONS

We show closed form expressions for the most common operations in the Poincaré ball, but we refer the reader to (Ungar, 2008; Ganea et al., 2018b) for more details.

Möbius addition. The *Möbius addition* of x and y in \mathbb{D}^n is defined as

$$x \oplus y := \frac{(1 + 2\langle x, y \rangle + \|y\|^2)x + (1 - \|x\|^2)y}{1 + 2\langle x, y \rangle + \|x\|^2\|y\|^2}. \quad (9)$$

We define $x \ominus y := x \oplus_c (-y)$.

Möbius scalar multiplication. The *Möbius scalar multiplication* of $x \in \mathbb{D}^n \setminus \{\mathbf{0}\}$ by $r \in \mathbb{R}$ is defined as

$$r \otimes x := \tanh(r \tanh^{-1}(\|x\|)) \frac{x}{\|x\|}, \quad (10)$$

and $r \otimes \mathbf{0} := \mathbf{0}$.

Exponential and logarithmic maps. For any point $x \in \mathbb{D}^n$, the exponential map $\exp_x : T_x \mathbb{D}^n \rightarrow \mathbb{D}^n$ and the logarithmic map $\log_x : \mathbb{D}^n \rightarrow T_x \mathbb{D}^n$ are given for $v \neq \mathbf{0}$ and $y \neq x$ by:

$$\exp_x(v) = x \oplus \left(\tanh \left(\frac{\lambda_x \|v\|}{2} \right) \frac{v}{\|v\|} \right), \quad \log_x(y) = \frac{2}{\lambda_x} \tanh^{-1}(\| -x \oplus y \|) \frac{-x \oplus y}{\| -x \oplus y \|}. \quad (11)$$

Gyro operator and parallel transport. Parallel transport is given for $x, y \in \mathbb{D}^n, v \in T_x \mathbb{D}$ by the formula $P_{x \rightarrow y}(v) = \frac{\lambda_x}{\lambda_y} \cdot \text{gyr}[y, -x]v$. Gyr^6 is the gyroautomorphism on \mathbb{D}^n with closed form expression shown in Eq. 1.27 of (Ungar, 2008):

$$\text{gyr}[u, v]w = \ominus(u \oplus v) \oplus \{u \oplus (v \oplus w)\} = w + 2 \frac{Au + Bv}{D}. \quad (12)$$

where the quantities A, B, D have closed-form expressions and are thus easy to implement:

$$A = -\langle u, w \rangle \|v\|^2 + \langle v, w \rangle + 2\langle u, v \rangle \cdot \langle v, w \rangle, \quad (13)$$

$$B = -\langle v, w \rangle \|u\|^2 - \langle u, w \rangle, \quad (14)$$

$$D = 1 + 2\langle u, v \rangle + \|u\|^2 \|v\|^2. \quad (15)$$

⁶https://en.wikipedia.org/wiki/Gyrovector_space